Coupled-channel analysis for vector charmonia and their nature

Satoshi X. Nakamura

[1] Institute of Frontier and Interdisciplinary Science, Shandong University, Qingdao, Shandong 266237, China

Graphical abstract

GraphicalAbstract content

Abstract

High-precision $e^+e^- \to c\bar{c}$ data (20 final states) from the BESIII and Belle in $\sqrt{s} = 3.75 - 4.7$ GeV are analyzed with a semi three-body unitary coupled-channel model. Vector charmonium poles are extracted from the amplitudes obtained from the fit. We find well-known ψ states listed in the PDG, and also several states near open-charm thresholds. The compositeness of the near-threshold poles suggests that $\psi(4040)$ could mainly consist of a $D^*\bar{D}^*$-molecule component, rather than a conventionally accepted quark-model $\psi(3S)$ state. Also, $\psi(4230)$ and $\psi(4360)$ might be substantial mixtures of $D_1(2420)\bar{D}$, $D_1(2420)\bar{D}^*$, $D_s^*\bar{D}_s^*$, and $c\bar{c}$ components.

Keywords

exotic hadrons; amplitude analysis; BESIII; heavy hadrons

1 Introduction

Recent BESIII measurements have accumulated high-quality e^+e^- annihilation cross sections for various final states covering wide energies. The measurements showed process-dependent lineshapes associated with exotic hadron candidates $Y(4230)$ and $Y(4360)$, and discovered charged charmonium-like $Z_c(3900)$ and $Z_c(4020)$. The process-dependent lineshapes invalidate the single-channel analysis (usual experimental analysis) to determine the vector charmonium properties such as the mass and width. We should analyze the data of different final states simultaneously with a unified

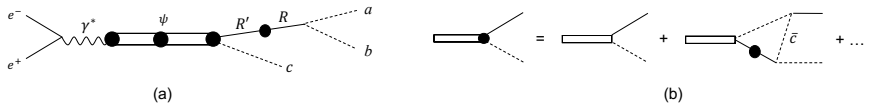

Figure 1: (a) $e^+e^- \to abc$ mechanism involving charmonium excitation. (Bare) two-meson resonances R and bare charmonium states are represented by the solid and double lines, respectively. Dressed propagators and vertices are indicated by the solid circles. (b) Direct and single triangle decay mechanisms of charmonium.

coupled-channel model that respects three-body unitarity. Such a coupled-channel analysis is the purpose of this work. The resonance properties obtained from the analysis set a primary basis to study the nature of exotic Y states. Furthermore, they are a prerequisite to explain how the process-dependent Y lineshapes come about. Also, for well-established charmonia [$\psi(4040)$, $\psi(4160)$, $\psi(4415)$], the coupled-channel analysis will provide new information because their properties were previously from a simple Breit-Wigner (BW) fit to the inclusive ($e^+e^- \to$ hadrons) data. We perform a coupled-channel analysis of the BESIII and Belle data over $\sqrt{s} = 3.75 - 4.7$ GeV for the first time, and show our fit and the vector charmonium pole locations. The full account of the analysis is given in Ref. [1].

The internal structures of the exotic candidates Y have been theoretically studied, and $Y(4230)$ [$Y(4360)$] as a $D_1\bar{D}$ [$D_1\bar{D}^*$] hadron molecule has been proposed [2, 3]. Our coupled-channel model has a freedom of generating the open-charm hadron molecules. By examining the compositeness [4], we explore the hadron-molecule contents in the vector charmonium states.

2 Coupled-channel model

We describe $e^+e^- \to c\bar{c}$ processes with an approximately three-body unitary coupled-channel model; see Ref. [1] for the full details. The full amplitude for the three-body

Table 1: Quasi two-body (Rc) coupled-channels.

$D_1(2420)\bar{D}^{(*)}$, $D_1(2430)\bar{D}^{(*)}$, $D_2^*(2460)\bar{D}^{(*)}$, $D^{(*)}\bar{D}^{(*)}$, $D_{s1}(2536)\bar{D}_s$ $D_s^{(*)}\bar{D}_s^{(*)}$
$J/\psi\eta$, $J/\psi\eta'$, $\omega\chi_{c0}$, $\Lambda_c\bar{\Lambda}_c$, $D_0^*(2300)\bar{D}^*$, f_0J/ψ, f_2J/ψ, $f_0\psi'$, f_0h_c, $Z_c\pi$, $Z_{cs}\bar{K}$

(abc) final states is given by

$$A_{abc,e^+e^-} = \sum_{abc}^{\text{cyclic}} \sum_{RR's_R^z} \Gamma_{ab,R}\,\tau_{R,R'}(p_c, E-E_c) \times \Big[\sum_{ij} \bar{\Gamma}^{\mu}_{R'c,\psi_i}(\boldsymbol{p}_c, E)\,\bar{G}_{ij}(E)\,\bar{\Gamma}_{\psi_j,\gamma^*}(E) + \bar{\Gamma}^{\mu}_{R'c,\gamma^*}(\boldsymbol{p}_c, E)\Big]\frac{l_\mu}{s}, \quad (1)$$

where the first and second terms in the square bracket are charmonium-excitation [Fig. 1(a)] and nonresonant (NR) parts, respectively. Cyclic permutations (abc), (cab), (bca) are indicated by $\sum_{abc}^{\text{cyclic}}$; $E(=\sqrt{s})$ denotes the abc invariant mass and $1/s$ is the virtual photon propagator; the lepton current matrix element is $l_\mu(= e\bar{v}_{e^+}\gamma_\mu u_{e^-})$; ψ_i indicates i-th bare ψ state. A particle x's mass, momentum, and energy are denoted by m_x, $\boldsymbol{p}_x$, and E_x, respectively. The symbol R is a two-meson resonance such as $D_1(2420)$, and $\Gamma_{ab,R}$ is $R \to ab$ vertex. The amplitude also includes quantities, dressed by quasi-two-body Rc continuum states, such as the Rc Green function ($\tau_{R,R'}$), the $\psi_i \to Rc$ vertex ($\bar{\Gamma}^{\mu}_{Rc,\psi_i}$), the NR Rc production vertex ($\bar{\Gamma}^{\mu}_{Rc,\gamma^*}$), the ψ production mechanism ($\bar{\Gamma}_{\psi_i,\gamma^*}$), and the ψ propagator ($\bar{G}_{ij}$).

We consider Rc channels summarized in Table 1. For unstable charmed mesons other than $D_0^*(2300)$, we use a BW form for $\tau_{R,R'}$, which causes the partial three-body unitarity violation. $D_0^*(2300)$, $f_{0(2)}$, and $Z_{c(s)}$ are poles in $L=0$ $D\pi$, $L=0(2)$ $\pi\pi - K\bar{K}$, and $J^{PC}=1^{+-}$ $D^*\bar{D} - D^*\bar{D}^* - J/\psi\pi - \psi'\pi - h_c\pi - \eta_c\rho$ ($J^P=1^+$ $D_s^*\bar{D} - D_s\bar{D}^* - J/\psi K$) coupled-channel scattering amplitudes, respectively.

The nonperturbative coupled-channel Rc scattering is driven by bare ψ-excitations, (on-shell) particle-exchanges, and short-range contact interactions, in a way to satisfy the three-body unitarity. The bare ψ states are then dressed by the Rc continuum states to form charmonium resonance states. Besides, the short-range contact interactions alone may generate hadron-molecule states.

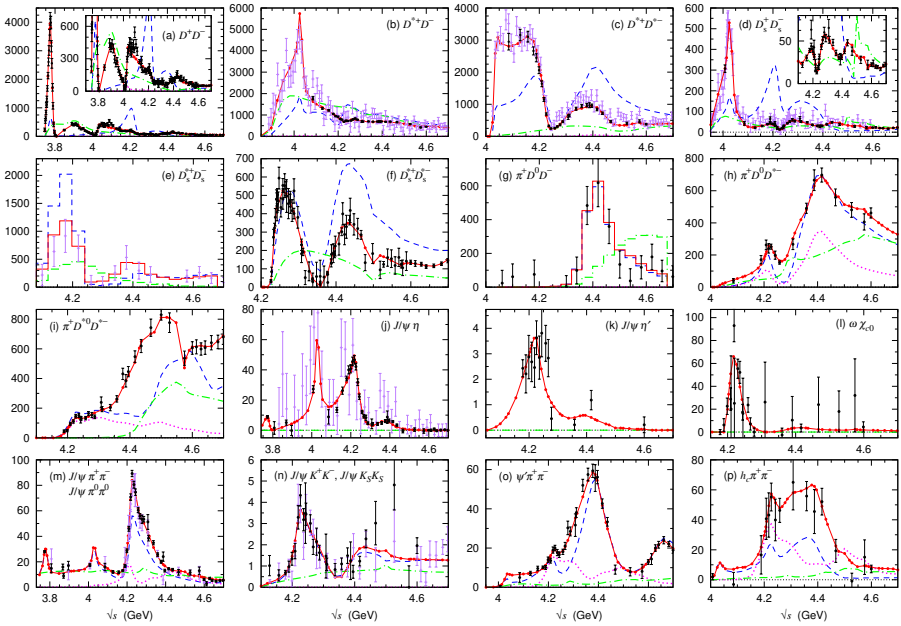

Figure 2: e^+e^- annihilation cross sections (unit:pb); each panel indicates the final state; $\sqrt{s}$ is the total energy. Full calculations are shown by the red points, connected by lines. The direct decays, single-triangle, and nonresonant contributions are shown by the blue dashed, magenta dotted, and green dash-dotted curves, respectively. Figures taken from Ref. [1] where references for the data are given.

3 Fit results

We fitted $e^+e^- \to c\bar{c}$ cross-section data (20 final states) as well as available invariant-mass distribution data. Five bare ψ states were needed for reaching a reasonable fit. Furthermore, we included $\psi(4660)$ and $\psi(4710)$ BW amplitudes to fit data for $\sqrt{s} \gtrsim 4.6$ GeV. With 200 fitting parameters, our default fit reached $\chi^2/\mathrm{ndf} = 2320/(1635-200) \simeq 1.6$.

Some of the fit results are shown in Fig. 2. For more fit results, see Ref. [1]. The default-fit results are shown by the red circles connected by lines. Also, contributions from the direct-decay and single-triangle rescattering mechanisms defined in Fig. 1(b) are shown by the blue-dashed and magenta dotted curves.

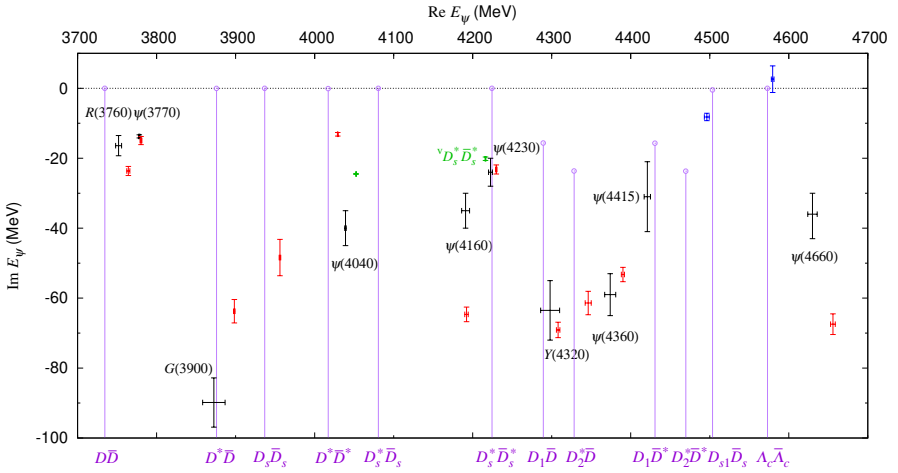

Figure 3: Vector charmonium poles (E_ψ) and their uncertainties. Red, blue, and green points indicate pole locations of resonances (located on unphysical sheets of open channels), bound, and virtual states, respectively; the bound (virtual) states are on the physical (unphysical) sheets of the nearest-threshold channels, respectively. Black points indicate ψ states listed in PDG [5], $\mathcal{R}(3760)$ [6], $G(3900)$ [7], and $Y(4320)$ [8]. Branch points (thresholds) and cuts for open-charm channels indicated at the bottom are shown by open circles and accompanying vertical lines, respectively. Figure taken from Ref. [1].

Remarks are in order: (i) The data show several cusp structures at thresholds such as: $D_1(2420)\bar{D}^*$ (4431 MeV) in Fig. 2(a); $D_1(2420)\bar{D}$ (4289 MeV) in Fig. 2(b); $\Lambda_c\bar{\Lambda}_c$ (4573 MeV) in Fig. 2(i). Our model generates these cusp structures with the short-range contact interactions. (ii) The short-range interactions generate hadron-molecule poles that cause significant threshold enhancements, as indicated by differences between the red solid and blue dashed curves in Figs. 2(a)-(f). (iii) As a consequence of the coupled-channel fit, our model creates common structures in different processes, even when not necessarily required by the data. For example, $\psi(4040)$ peaks appear in $D^*\bar{D}$ [Fig. 2(b)] and $D_s\bar{D}_s$ [Fig. 2(d)] to fit the data, and they also appear in others [Fig. 2(j,m,o,p)] for which data are lacking at the peak. (iv) The $J/\psi K^+K^-$ data

[Fig. 2(n)] show an enhancement suggesting $Y(4500)$ [9]. However, our model does not fit it since the data is rather fluctuating in this region, and the $J/\psi K_S K_S$ data does not indicate the same enhancement.

4 Vector-charmonium poles and compositeness

The coupled-channel amplitude obtained from the fit is analytically continued for searching vector charmonium poles E_ψ on unphysical sheets of the open channels and physical sheets of the closed channels, or slightly deviated from this condition. The range is $3.75 < M < 4.7$ GeV ($M \equiv \mathrm{Re}[E_\psi]$), and $\Gamma \equiv -2 \times \mathrm{Im}[E_\psi] < 0.2$ GeV.

Fourteen states are found, as shown in Fig. 3 along with experimental analysis results. Compared to the uncertainties estimated in the experimental single-channel analyses, our pole uncertainties are generally smaller. This is probably because our pole values are constrained by the data of the various processes and some of the data are very precise. Our result includes all the counterparts of the vector charmonium states ($M > 3.75$ GeV) listed in the PDG [5], although sizable differences can be seen such as the $\psi(4040)$ width and the $\psi(4415)$ mass and width. Actually, the $\psi(4040)$, $\psi(4160)$, and $\psi(4415)$ resonance parameters in the PDG are from a simple BW fit to the R values [10]. Such a simple analysis could have caused artifacts in the resonance parameters. More states are found near the open-charm thresholds. Those located near the $D_s^{(*)}\bar{D}_s^{(*)}$ and $D_{s1}\bar{D}_s$ thresholds are found for the first time in the present analysis.

We calculate the compositeness [4] of the poles as a qualitative measure of the internal structure. A continuum (two-body) Rc channel content in a state is denoted by X_{Rc} (compositeness) and, combined with an elementariness Z_a of a bare state a, it satisfies $\sum_{Rc} X_{Rc} + \sum_a Z_a = 1$. However, it is noted that the compositeness should be viewed with caution because X_{Rc} is generally complex and its imaginary part and negative real part are difficult to interpret. Also, the X_{Rc} also depends on the choice of the form factors.

In Tables 2, we present the compositeness for some of the vector charmonium states shown in Fig. 3. Some states have large compositeness. It is interesting to find that

Table 2: Compositeness X_{Rc} of some of vector charmonium states shown in Fig. 3. Hyphens indicate $|X_{Rc}| < 0.01$. Table taken from Ref. [1].

$Rc \setminus \psi$	$\psi(4040)$	${}^{\rm v}D_s^*\bar{D}_s^*$	$\psi(4230)$	$\psi(4360)$
$D\bar{D}$	–	–	–	–
$D^*\bar{D}$	$-0.01+0.01i$	–	–	–
$D^*\bar{D}^*$	$0.86+0.22i$	$0.01+0.02i$	–	–
$D_1\bar{D}$	–	$0.23-0.12i$	$0.18+0.13i$	$0.31-0.06i$
$D_1\bar{D}^*$	–	$0.04-0.06i$	$0.09+0.05i$	$0.29-0.16i$
$D_2^*\bar{D}^*$	–	$0.02-0.01i$	–	–
$D_s^*\bar{D}_s^*$	–	$0.50+0.25i$	$0.35-0.27i$	–
Sum	$0.86+0.19i$	$0.83+0.12i$	$0.65-0.13i$	$0.61-0.27i$

the well-established $\psi(4040)$ has $X_{D^*\bar{D}^*} = 0.86$. Conventionally, this state has been assigned to the quark-model $\psi(3S)$ state as an input to determine the quark-model parameters. Our result might be casting a doubt to this conventional practice. In literature [2, 3], it has been argued that $\psi(4230)$ and $\psi(4360)$ can be $D_1(2420)\bar{D}$ and $D_1(2420)\bar{D}^*$ molecules, respectively. However, our result suggests more complex structures. Due to the coupled-channel dynamics, molecular states [$D_1(2420)\bar{D}$, $D_1(2420)\bar{D}^*$, and $D_s^*\bar{D}_s^*$] and also bare ψ states are substantially mixed in $\psi(4230)$, $\psi(4360)$, and ${}^{\rm v}D_s^*\bar{D}_s^*$ states.

5 Summary

A global coupled-channel analysis of most of the available $e^+e^- \to c\bar{c}$ data (20 final states) in $\sqrt{s} = 3.75 - 4.7$ GeV was performed. Reasonable fits were obtained for both cross-section and invariant-mass distribution data. We extracted vector-charmonium poles including not only familiar vector charmonia, but also those near the open-charm thresholds. The compositeness of the states suggested that open-charm hadron-molecular structures dominated in many states. The $\psi(4230)$ and $\psi(4360)$ states are not simple $D_1\bar{D}$ and $D_1\bar{D}^*$ molecules, respectively, but are the mixtures of $c\bar{c}$ and $D_1\bar{D}$, $D_1\bar{D}^*$, and $D_s^*\bar{D}_s^*$ molecules. A large $D^*\bar{D}^*$ compositeness

in $\psi(4040)$ was also suggested.

References

[1] S.X. Nakamura, X.-H. Li, H.-P. Peng, Z.-T. Sun, and X.-R. Zhou. Global coupled-channel analysis of $e^+e^- \to c\bar{c}$ processes in $\sqrt{s} = 3.75$ to 4.7 GeV. **2025**, *Phys. Rev. D, 112*: 054027.

[2] T. Ji, X.-K. Dong, F.-K. Guo, and B.-S. Zou. Prediction of a Narrow Exotic Hadronic State with Quantum Numbers $J^{PC} = 0^{--}$. **2022**, *Phys. Rev. Lett., 129*: 102002.

[3] F.-Z. Peng, M.-J. Yan, M. S. Sánchez, and M.P. Valderrama. Light- and heavy-quark symmetries and the $Y(4230)$, $Y(4360)$, $Y(4500)$, $Y(4620)$, and $X(4630)$ resonances. **2023**, *Phys. Rev. D, 107*: 016001.

[4] T. Sekihara, T. Hyodo, and D. Jido. Comprehensive analysis of the wave function of a hadronic resonance and its compositeness. **2015**, *PTEP, 2015*: 063D04.

[5] R.L. Workman et al. (Particle Data Group). Review of Particle Physics. **2022**, *Prog. Theor. Exp. Phys., 2022*: 083C01.

[6] M. Ablikim et al. (BESIII Collaboration). $\mathcal{R}(3780)$ Resonance Interpreted as the 1^3D_1-Wave Dominant State of Charmonium from Precise Measurements of the Cross Section of $e^+e^- \to$ Hadrons. **2024**, *Phys. Rev. Lett., 133*: 241902.

[7] M. Ablikim et al. (BESIII Collaboration). Precise Measurement of Born Cross Sections for $e^+e^- \to D\bar{D}$ at $\sqrt{s} = 3.80 - 4.95$ GeV. **2024**, *Phys. Rev. Lett., 133*: 081901.

[8] M. Ablikim et al. (BESIII Collaboration). Study of the resonance structures in the process $e^+e^- \to \pi^+\pi^- J/\psi$. **2022**, *Phys. Rev. D, 106*: 072001.

[9] M. Ablikim et al. (BESIII Collaboration). Observation of the $Y(4230)$ and a new structure in $e^+e^- \to K^+K^- J/\psi$. **2022**, *Chin. Phys. C, 46*: 111002.

[10] M. Ablikim et al. (BES Collaboration). Determination of the $\psi(3770)$, $\psi(4040)$, $\psi(4160)$ and $\psi(4415)$ resonance parameters. **2008**, *Phys. Lett. B, 660*: 315.